IOP Publishing Measurement Science and Technology
Meas. Sci. Technol. **31** (2020) 042002 (16pp) https://doi.org/10.1088/1361-6501/ab5f71

Topical Review

A review of state-of-the-art 1D length scale calibration instruments

Tim Coveney

National Physical Laboratory, Hampton Road, Teddington, Middlesex, TW11 0LW, United Kingdom

E-mail: tim.coveney@npl.co.uk

Received 21 June 2018, revised 26 November 2019
Accepted for publication 6 December 2019
Published 14 January 2020

Abstract

The high-level dissemination of the SI unit of length, the metre, relies on primary level 1D length measurement instruments to calibrate transfer standards for measurement users. The majority of these instruments are maintained by National Measurement Institutes and the instrument designs vary significantly. Certain application-specific design challenges are common to all of these instruments which have been overcome using many innovative and original approaches by different researchers. This review will discuss what some of these application specific design challenges are in the context of primary level 1D length measurement and review details of the solutions that have been made available in literature. Finally, the review will discuss the implications of any commonalities or wide variations in approach to the different design challenges, with a view to providing a starting point for future instrument designers.

Keywords: dimensional measurement, instrument design, length, interferometry

(Some figures may appear in colour only in the online journal)

1. Introduction

The metre is one of the seven base units of the International System of Units (SI) and as such both accurate realisation and dissemination of the metre are crucial to achieving accuracy in measurements across many fields [1]. Because the definition of the metre is based on the speed of light, the primary methods of realising the metre all rely on electromagnetic radiation, either via the frequency of the wave or by time of flight [2, 3]. However, most standards used for length metrology in the macroscale range (lengths of the order 1 mm to 2 m) are material standards of various types. Commonly used standards for linear dimensions include gauge blocks [4], length bars [5] and step gauges [6, 7]. Internal and external diameter standards, such as plain setting rings and plugs are also widely used [8, 9]. These must be calibrated against the primary realisations of the metre to ensure traceability of measurement. These calibrations are typically carried out within National Measurement Institutes (NMIs) or specialised calibration laboratories. Given the specialised nature of the instrumentation designed to perform such calibrations, most laboratories have produced their own bespoke systems. While each of these instruments has unique features, the tasks they are designed to achieve are the same and there are common error sources which must be addressed to achieve the desired accuracy.

This review will explore what these common error sources are (though not exhaustively), then discuss the various solutions that different institutes have adopted to eliminate or correct for them. The overall performances of the systems will not be compared, but the strengths and weaknesses of the different approaches reported will be discussed. In the case of NMIs signatory to the CIPM Mutual Recognition Arrangement, details of their internationally recognised calibration and measurement capabilities (CMCs) can be found online in the BIPM key comparison database (KCDB) [10].

2. Common error sources

The design of every measurement system will have its own individual weaknesses or design compromises that will lead to unique errors which must be addressed in some way to maximise accuracy and minimise uncertainty. For NMI level calibration systems the reduction of uncertainty to a minimum value is critical and it is often the primary design consideration. Although there is no formal or generally agreed definition of what NMI level performance in length calibration is, a useful benchmark is to state that to be classified as being of high or NMI level accuracy, length measuring systems will aim to achieve an uncertainty equivalent to less than 1 μm for a 1 m long measurand ($k = 2$). The best systems will achieve uncertainties less than half this with the lowest reported uncertainty for a macroscopic length being that reported for the PTB nanometer comparator; equivalent to 10 nm for a 1 m length (although this instrument has only a 610 mm maximum range) [11]. To achieve uncertainties at this level, given the wide range of possible error sources, it is necessary to account for errors at levels down to 1 nm or less which would often be considered negligible in other systems. Errors of the order of 100 nm must certainly be accounted for and generally corrections will be required with the residual uncertainty after correction (the uncertainty *of* the correction) forming the final contribution.

As previously noted, each system design will have unique sources of error, and where the source is common different systems will vary in their sensitivity to each error. Therefore, different designers may regard the same error source as significant or negligible depending on their particular design approach or measurement challenge. However, there are a number of sources of error which relate to fundamental principles of dimensional metrology which all systems will have to account for in some way. While the principles themselves are fundamental, there are many possible ways of eliminating, minimising or compensating for the errors and different approaches will be taken by different designers to suit different design philosophies. An exploration of the nature of five of these fundamental error sources follows.

2.1. Abbe principle

The Abbe principle, named after Ernst Abbe, states that, in the ideal setup, a length measuring instrument should be constructed such that the distance to be measured is a straight-line extension of the reference scale. Where this is not the case, the length indicated by the instrument will only be equal to the true length of the measurand (assuming no other sources of error) when the motion system of the instrument moves parallel to the line of the reference scale. If any rotation occurs during the motion between the initial and final positions of the measurement line then the indicated length will be different from the true length [12].

Ernst Abbe described methods to avoid the error incurred by mechanical design [13] and the difference between scale reading and measured length is known as the Abbe error. In an ideal length measurement system this error is absent but often practicalities, or the form of the artefact to be calibrated, make achieving this difficult, or impossible.

Where it exists, the consequence of the Abbe error is to create a difference between the length of the measurand and the scale reading of the measurement instrument. This error is dependent on both the Abbe offset, that is the spatial separation between the measurement line and the position to be measured, and the allowed magnitude of rotations in the system. These rotations can come from imperfections in the straightness of the motion of the measurement system from one position to another or from the rotation or elastic bending of the probing system which determines the location of the position to be measured. In fact, the source of the rotation does not affect the error, though determining it is important for managing the magnitude.

The magnitude of the resultant error in measured length δL can then be determined from the following equation:

$$\delta L = A_{\text{off}} \times \tan\theta$$

where A_{off} is the Abbe offset and θ is the angle of rotation. Since θ is expected to be small, a small angle approximation can be made so that

$$\delta L \approx A_{\text{off}} \times \theta.$$

To minimise the error both the Abbe offset, and the allowed magnitude of rotation need to be minimised. If either can be made zero, then the error is removed entirely. Practically this is virtually unachievable since even if the system can be designed such that the measuring scale and the measurement axis of the measurand are co-linear (an idealised Abbe system) imperfections in the motion will have the effect of creating a small offset. Therefore, when considering the Abbe principle with regard to precision instrument design the objective is to minimise the produced error, whether through design or through corrections applied, rather than fully eliminating it.

A key part of minimising Abbe error is the configuration of the laser interferometry systems utilised to measure the length of the artefacts under calibration. Laser interferometers are the principle embodiment of the realisation of the metre used over the macroscale distance and a variety of optical layouts are used. The different configurations open up different approaches to dealing with Abbe error.

2.2. Motion induced errors

For all but the simplest length standards (gauge blocks or length bars) some form of motion is needed to bring the probing mechanism to successive measurement positions. It is not always necessary to move the probe to achieve this, the artefact can be moved or any combination of movements that bring probe and measurement positions together. This motion must be straight relative to the measurement axis of the artefact to avoid cosine errors. Angular errors which affect the straightness of motion are common in motion systems, especially if there are multiple motion axes present and instrument design must seek to minimise these or compensate for their effects.

The highest accuracy systems for gauge blocks and length bars carry out interferometry directly between the two faces by wringing a platen to one end, thus avoiding the need for movement.

Consideration must be given to how to achieve repeatable and accurate position of the probing system over long distances.

2.3. Refractive index compensation

Realising the metre by either time of flight of a light ray or by standard frequency methods via laser interferometry requires the user to correct for the effect of the refractive index of the medium through which the light travels, typically air. In practice, time of flight measurements are rarely useful over the macroscale range due to the difficulty of measuring the extremely short time intervals involved (a return trip of 1 m would take a light ray approximately 7 ns, a trip of 10 mm would take 70 ps) [2]. Therefore, only the effect of refractive index on interferometry will be explored.

The refractive index correction is required because the SI definition of the metre defines the speed of light in a vacuum c. Since c is the constant that relates the frequency and the wavelength of an electromagnetic wave it follows that the wavelength of the laser (the scale of the interferometer) derived either from a calibrated frequency or from the CIPM List of recommended frequency standard values [3] will be the vacuum wavelength. Since the wavelength of light in a medium will differ from its wavelength in vacuum in proportion to the inverse of the medium's index of refraction the scale interval of the interferometer will be incorrect if the vacuum wavelength is used. Therefore, the refractive index of the medium must be measured in order to correct the wavelength and therefore the measurement scale.

Since the refractive index of air during a precision length measurement can be variable to a significant degree this is non-trivial. It is also true that since air is a mixture of varying quantities of a number of different gases it is not possible to define a straightforward value for its refractive index, as can be done for pure gases.

As an illustration consider a simple linear homodyne interferometer operating at the recommended vacuum wavelength of an un-stabilised helium-neon laser, $\lambda_{\mathrm{He-Ne}}$ which is given as 632.9908 nm [14].

The length measured by an interferometer, L, is given by

$$L = \frac{N\lambda}{2}$$

where N is the number of fringes observed by the counter system of the interferometer, and λ is the wavelength of the light in the medium through which it travels. Unless this is vacuum then the wavelength of light will be reduced from its vacuum wavelength, λ_0, in proportion to the refractive index of the material n:

$$\lambda = \frac{\lambda_0}{n}.$$

Then L is given by

$$L = \frac{N\lambda_0}{2n}.$$

A typical value for refractive index of air under standard conditions is 1.000 271. As an example of the effect of an incorrect value for refractive index being assumed, if a length of 1 m is measured at standard conditions and then again after the environmental conditions have changed such that the refractive index has changed by 1×10^{-6} but without making the necessary correction the measured length will change by approximately 1 μm. A rough guide to individual environmental parameters changes which could cause a 1×10^{-6} change in refractive index would be a 1 °C temperature change (less than typical diurnal temperature variation which may be 10 °C or more in some areas), a change in air pressure of 3.7 hPa (the difference between high and low barometric pressure on either side of a weather front in Europe may be up to 30 hPa or 3000 Pa), or a change of 80% in relative humidity [15]. The change in carbon dioxide concentration required to cause a similar change in refractive index would be greater than could be expected to be encountered in a standard laboratory environment. Smaller variations of several parameters combined would have the same effect. Errors of this magnitude would need to be corrected to achieve the uncertainties required for primary level instruments.

An alternative approach is to run the laser through an evacuated path, removing the issue of refractive index altogether. However, since the length of any material standard would change if it were placed in a vacuum due to the removal of atmospheric compression, some form of linkage between the evacuated path and the artefact in air is required in this case. This presents an engineering challenge to the system designer in addition to the challenges of maintaining vacuum over a practical path length.

2.4. Effective probe diameter and compression effects

Where contacting probes are used to fiducialise the measurement position and measurements are made bi-directionally, the size of the probe must be accounted for. In most systems of this type the probe will be spherical to give a point contact on the measurement surface, though in some cases other geometric forms may be used, such as a cylindrical probe. The diameter of the probe will appear as erroneous additional length on faces probed in the opposite direction to the datum face so must be measured and subtracted from these results. In addition, compression effects will need consideration depending on the means used to measure the probe size.

Also, to be considered here is the compression of the measurement face when probed. In order to avoid damage to artefacts, probing forces should always be low enough that such compression is within the elastic limits of the materials to be probed. However even this elastic compression can be sufficient to be an error of noticeable magnitude. In the case of a 5 mm diameter ruby ball contacting a steel flat surface (a

common probing case for dimensional systems generally) if the probing force is 0.5 N the resultant compression, according to the equations in case 2 derived by Puttock and Thwaite [16] will be 139 nm. This is significant in the context of primary measurements where total systemic uncertainties will be of the same order as this error.

2.5. Temperature measurement and control

The biggest limiting factors on the achievable uncertainty of dimensional measurement are usually the stability of temperature and the accuracy with which it can be measured.

Varying temperature will affect the refractive index of the laser path where this is not in vacuum, and this will lead to changes in the measured length of the artefact. In addition, the physical dimensions of all but a handful of low thermal expansion materials vary with temperature in accordance with the material's coefficient of thermal expansion.

To allow the meaningful comparison of length measurements made in different times and places ISO 1:2016 [17] states that

> The standard reference temperature value for the specification of geometrical and dimensional properties shall be fixed at 20 °C.

This means that for a dimensional standard, the calibrated result must be the value of length the artefact would be if it were at the reference temperature of 20 °C during measurement. Since this is unlikely to be the case during an actual calibration, thermal expansion corrections are generally required. Making thermal expansion corrections requires knowledge of the actual material temperature during measurement and the thermal expansion coefficient of the material used. The residual uncertainties from this correction come from the uncertainty with which these two values can be determined. Minimising the uncertainties from the thermal expansion correction therefore requires: low uncertainty measurements of the material temperature; temperature control to keep the ambient temperature close to 20 °C so that the size of correction required is small; and an accurate value for the coefficient of thermal expansion.

It should be noted that the thermal expansion uncertainty terms reduce significantly (to almost nothing) if the artefact to be measured is made of a low thermal expansion material, for example ZERODUR® [18] Invar or Super Invar. Most of the lowest uncertainty CMC claims for macroscale length in the KCDB require that the artefact to be measured be made of a low expansion material. While from a purely metrological point of view such standards are desirable, in practice it is often better to manufacture transfer standards from the same material as the item which will be measured by the device to be calibrated as this minimises errors going forward. For this reason, as well as for reasons of cost and mechanical stability (especially Invar, see Berthold *et al* [19]), low thermal expansion material length standards are comparatively rare and the majority of material standards used as first level transfer standards are manufactured from steel, with some being manufactured from tungsten carbide and a smaller subset manufactured from ceramic materials.

Thermal expansion can also affect the geometry of the measuring instrument, especially if the geometry is asymmetric as is often the case. Here again, low thermal expansion materials can used though the same cautions as with length standards apply. Combining materials can also minimise thermal expansion if the structure can be built such that expansions of different materials can compensate for each other. Either of these approaches adds to the manufacturing costs and design difficulties. A more common approach is to place the instrument into a temperature-stabilised environment, either an enclosure or a laboratory.

3. Systems in service

Details of all systems that take part in key comparisons as part of the CIPM MRA are included in the published reports of those comparisons. The following sections will draw from these reports in addition to published accounts of systems in journals and conferences, and will review the various solutions that have been developed for each of the common error sources listed above.

3.1. Minimising Abbe error

Both Bryan [20] and Zhang [21] have published work re-exploring the concept of Abbe error and designing to minimise it in dimensional systems.

The ideal way to minimise Abbe error in a measurement system is to have co-linear artefact measurement lines and instrument measurement paths. For gauge blocks and length bars measured by direct face interferometry this can be the case. Instruments that work in this way include the NPL Primary length bar interferometer [22], PTB's next generation Kösters interferometer [23], the double ended interferometer reported by Rau *et al* [24] and the NPL-TESA gauge block interferometer, a widely used commercially available primary instrument that been progressively upgraded since its introduction in 1986 [25–27]. In these instruments Abbe error can be said to be minimised provided the alignment of the optical axis of the interferometer to the measurement axis of the gauge is ensured. This can be achieved because the opening out of the interference fringe to give a uniform field across the surface of the platen ensures that the normal to the platen (i.e. the defined measuring axis of the gauge) is aligned with the normal to the interferometer reference mirror. Correct alignment of the reference mirror is assured by autocollimation of the beam back to the input fibre face. As a result, the limitation on how far Abbe error can be reduced on instruments of this type is often the straightness and parallelism of the standards rather than the design of the instrument.

However, gauge blocks and length bars are a special case of dimensional standard due to their lapped flat faces. These grant the metrologist the ability to wring a platen to the reverse face, allowing measurement by direct face interferometry. This is not the case for most common dimensional standards,

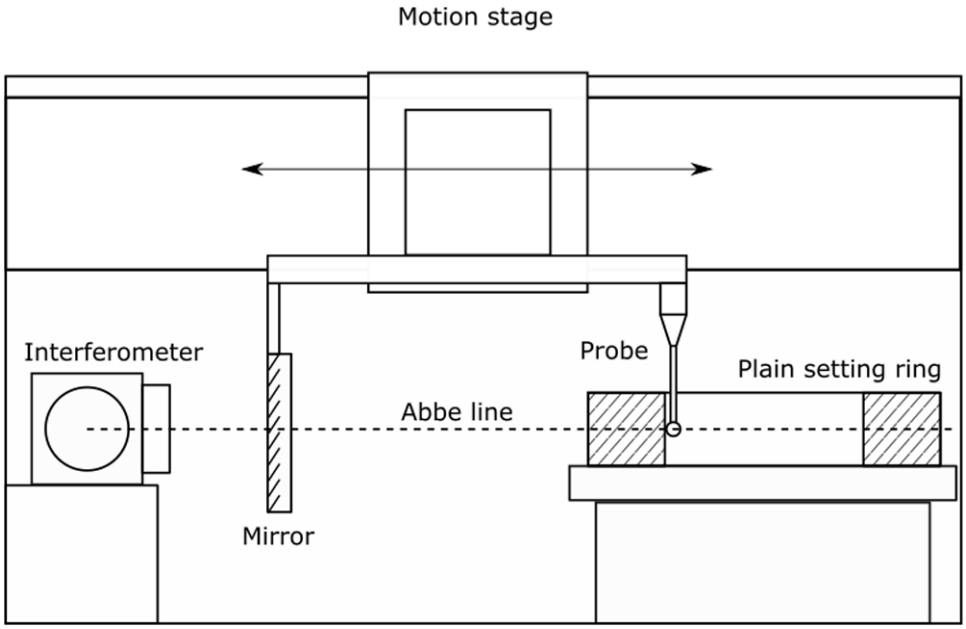

Figure 1. Simplified view of the KRISS Abbe-type comparator measuring a plain setting ring, showing the co-linearity of the probe and interferometer. For clarity the ring is shown in section view.

for example it would be impossible to wring a platen of sufficient size to the curved measurement faces of diameter standards. Here minimising or compensating for Abbe error involves significant amounts of design ingenuity.

For shorter standards one approach is to mechanically link the distance to be measured to a distance in free space outside the standard which can be measured, typically using a laser interferometer. The optical axis of the measurement arm of this interferometer is designed to pass through the centre of the contacting probe. Thus, the probe and the measurement scale (the interferometer) are in the same line and the Abbe error is minimised. An illustration of this layout, as used by Kim *et al* [28] at the South Korean NMI KRISS is shown in figure 1. A similar layout is adopted on the NPL Internal Diameter Machine [29] though here the principal motion is made by moving the artefact being measured with the probing system on an air slide and it is the interferometer block rather than the moving mirror which is mechanically linked to the probe. The moving mirror on the NPL system is attached to the motion table, giving the advantage that once the ring has contacted the probe the distance between the interferometer and the mirror remains constant if the stage travels through the desired contact point (assuming that the bend of the stylus does not become significant).

This mechanical bridging fulfils the Abbe criteria and can also allow the position of the measuring line of the artefact to be varied, for example to explore the diameter variation at different heights within the bore of a plain setting ring, provided that it is the artefact which changes position, independently of the position of the probe and interferometer components. A limitation of this approach is that it requires the instrument to be at least double the length of the maximum dimension to be measured, making it impractical for larger artefacts. This limitation is further enforced by the fact that the mechanical linking structure needs to be as free as possible of mechanical deformation due to gravity. The longer the structure, the more difficult it becomes to achieve this, potentially increasing the weight of the structure and putting stress on the ability of the motion system to provide precision positioning. Thermal variation may also be of concern as the thermal expansion of the linking structure will cause the measured length to vary, typically in opposition, and with a different magnitude, to the artefact. Additionally, in a design similar to that shown in figure 1 the linking structure will act as a lever, magnifying the effect of motion errors, most significantly rotation around the *Y* axis or pitch. This effect will worsen with length, again potentially limiting the layout to shorter lengths.

Another arrangement for minimising Abbe error is to place the interferometer in line with the axis of measurement of the artefact but separate from the motion stage. An illustration of a system of this type can be seen in figure 2. A reflector (a plane mirror or a corner cube could be used) is placed at the end of the gauge and the motion of the stage measured. A probing system acts as a fixed point to which each desired measurement position is referenced and the displacement of the stage between each measurement position is measured and recorded as the measurement result.

Specific examples of this layout include a modified SIP F1A length measuring machine used for step gauge measurement at LNE [30] and the Laser automatic interferometric comparator (AIC) developed at NIM [31]. This layout has the same limitation as the use of a mechanical linkage in that it requires a length in free space between the reflector and the interferometer at least as long as the length of the maximum artefact to be measured. Indeed these layouts could be seen as a form of mechanically linked system where the machine table is the mechanical link rather than the probing structure (as in the instruments in [28, 29]). However, linking through the table incurs less of the risks associated with deformation and bending since the structure can be significantly stronger

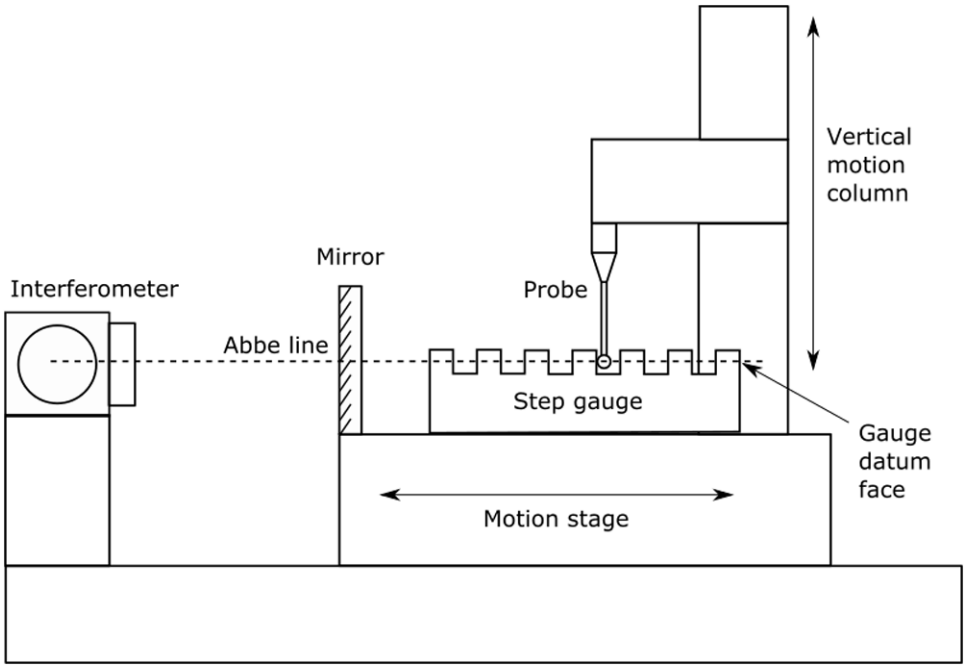

Figure 2. An illustration of a motion stage displacement measuring system. The interferometer is zeroed with the probe in contact with the gauge datum face and the displacement of the stage as the probe touches each subsequent face is equal to the face separation.

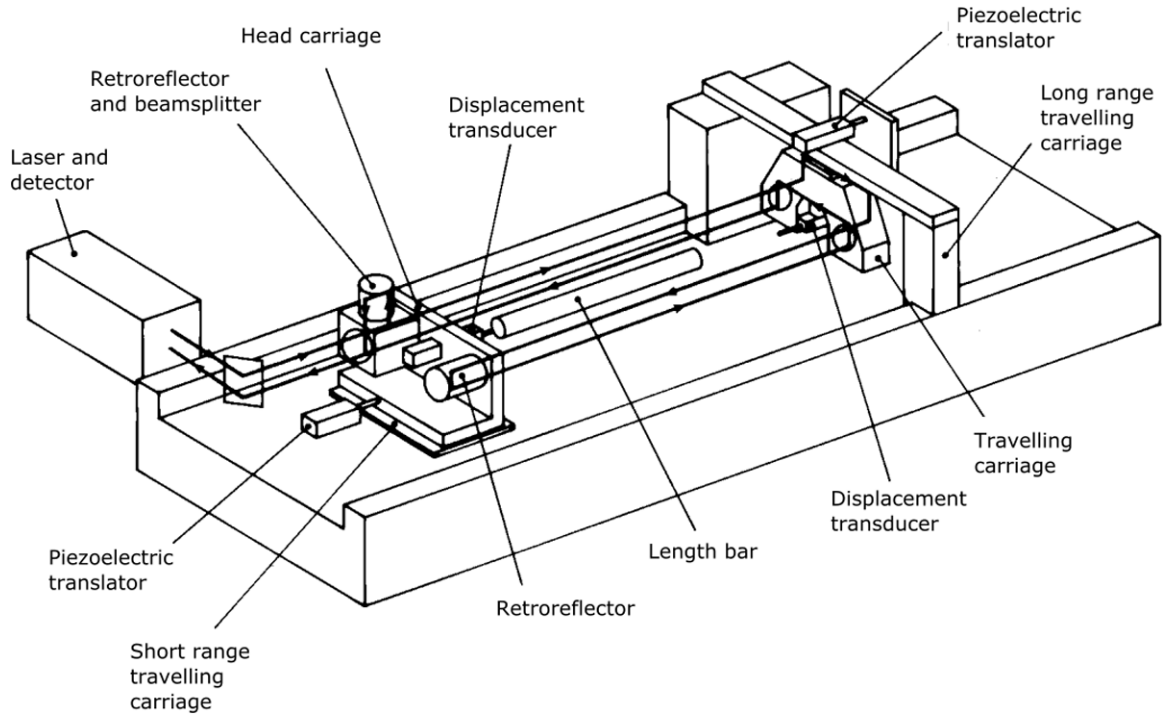

Figure 3. The NPL Length Bar Machine, showing the symmetrical distribution of beam paths around the measurement axis.

due to the lower criticality of weight here. Abbe errors are minimised by this layout assuming co-linearity of the motion and the interferometer axis. Motion or alignment errors can thus lead to an increase in the Abbe error observed. In particular, if the probe is not repositioned repeatably on the vertical motion column then an Abbe error will be introduced.

In some cases, however, it is not possible for the interferometer and probe to be in a single line. Here then the Abbe error is not minimised and may be significant. Means must be sought to correct for the error, either by quantifying it and applying a numerical correction to the resultant length or by designing a system that self corrects the error due to its configuration.

To do the latter, the designer can choose to use multiple laser axes placed symmetrically around the probing axis. This can be seen in figure 3, the NPL Length Bar Machine which uses this type of 'wrap-around' system to minimise the Abbe error. Provided the beam paths are symmetrical around the

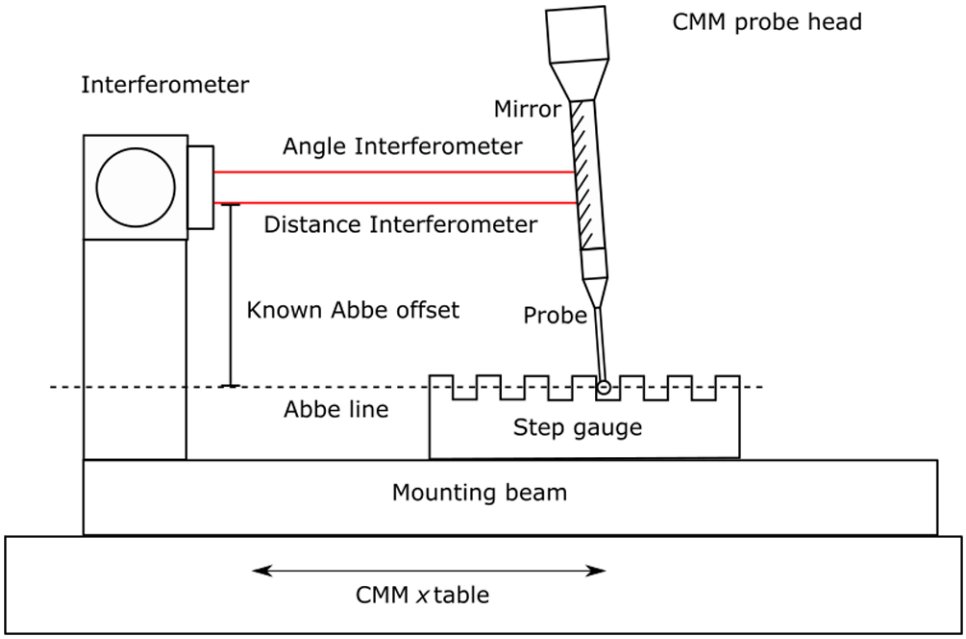

Figure 4. Simplified layout of the NPL Step Gauge Rig 1. The tilt of the probe is exaggerated.

contact point of the probe and the beam reflectors form a plane which includes the probe position, rotation of the structure will result in an equal and opposite change in the observed lengths recorded by the separate interferometer axes (in the absence of other factors affecting the measurements differently) and averaging the readings will give the length that would be observed if no rotationally induced Abbe error had occurred. In practice, mechanical deformation of the structures or the thickness of the probe will still cause small Abbe errors which may need to be accounted for in a primary length calibration system.

Another example of a system of this type is the Step Gauge Interferometer developed by Byman *et al* [32] at VTT-MIKES, the Finnish NMI. The probing head carries two corner cubes, with the apexes vertically aligned with the centre of the probe tip and symmetrical around the vertical axis of the probe. This alignment means that the requirement for the reflectors to be in plane with the probe position is met, even though the corner cubes are non-planar devices. As a result, the optical arrangement of the instrument is insensitive to rotation.

A similar technique is reported by Picotto *et al* on the INRIM 1D comparator [33]. Here plane mirrors are used with the interferometer axes symmetrical around the vertical axis of the probe and in the same horizontal plane as the probe tip. This gives insensitivity to rotation, but the system is potentially affected by pitch introducing a cosine error due to the mirror and the incoming beam no longer being perpendicular.

Other systems using comparable design approaches include Kruger's modified length bar machine at NMISA [34], which uses plain mirrors and a four-pass interferometer arrangement. This provides the additional advantage that both pitch and yaw angles can be measured, since the interferometer beams are distributed symmetrically around the probe both horizontally and vertically. This allows corrections for small second order effects to be made, if the size of any small Abbe offsets due to mechanical deformation or probe thickness are present. Prieto and Rodriguez on the CEM-TEK 1200 interferometric comparator at CEM also use a symmetrical pair of plane mirrors [35].

Eom *et al* [36] use a similar arrangement for the KRISS universal end standard calibration system, with plane mirrors and interferometer beams symmetrically distributed around the probe tip. However, this system includes an additional interferometer measuring the angle of the mirrors to correct for the Abbe offset between the probe point and the rotational centres of two tilt stages. In practice, measured angular motion during calibration is usually less than 1 arc second due to a coupling between the angular compensation of each motion axis and a translation motion with the opposite sign.

The five optical configurations outlined above all allow the Abbe error to be minimised. However, the need for multiple axes can be limiting over longer ranges if the output power of the laser is limited. Also, the need to mount multiple reflectors requires additional supporting structure mass, which can be a limiting factor depending on the mechanics of the system. Some drive units or support structures, for example the probing head of a co-ordinate measurement machine (CMM), which are commonly used as a motion base for linear calibration systems, may have a weight limit. In this case the multiple axes/reflectors design approach may not be suitable.

A third approach is to accept an Abbe error but quantify it and apply appropriate corrections. The NPL Step Gauge Rig 1 [30] is designed with the laser beam directly above the centre of the measurement line, offset from it by a known distance as shown in figure 4. A single plane mirror is mounted in a custom CMM probe mount. A combined distance/angle interferometer is used to measure the distance to the mirror and the angle of its tilt. The tilt is assumed to be imposed

by the probing action. The known vertical offset between the distance axis and the probe centre is used with the tilt angle to calculate a correction term which is applied to the measured length.

The NPL Step Gauge Rig 1 setup has the advantage that only a single reflector is required saving weight and allowing a more compact design. The close proximity of the two beams minimises differences caused by varying airflow or refractive index. The key disadvantage is that the method has a higher uncertainty contribution owing to the differing effects of uncertainty sources on the measured length and the measured angle.

The PTB nanometer comparator has a similar approach to that of the NPL system [37–40], using three reflectors mounted on the bridge to correct for both dilatation and bending within the system. An advanced method for determining and correcting for Abbe errors applied to the PTB nanometer comparator was reported by Köning *et al* in 2007 [41]. This involved inducing the error in a controlled way to quantify it. Lengths measured by the interferometers on the system were compared to a reference linear encoder. Piezo actuators driven by a sinusoidal signal were used to vary the pitch angle of the interferometer reflector mounts but not the reference encoder. The magnitude of the difference thus induced between the encoder and interferometer lengths could then be used to calculate an appropriate correction for the Abbe error. This correction was demonstrated to be effective at the nanometre level but required significant additional hardware and control systems to implement.

3.2. Accurate motion control methods

The selection of the motion system to be used for a primary 1D instrument is often key to its whole design since it will generally be the single largest component (in physical dimensions at least) unless the maximum range of the system is short. As such it is often the component that the rest of the system is designed around.

The key requirements for the measurement axis motion system in a primary length measurement application are its positioning resolution (although this need not be as small as the overall measurement resolution), the geometry of its motion (which should be straight and parallel with the measurement axis), the minimising of pitch and yaw, and the ability to maintain a stable position while measurements are taken. A further requirement may be that the motion system should not generate heat within the working volume. This can be accomplished by making the drive system remote, by insulating it or by selecting a drive unit with a low heat output.

Where other subsidiary axes of motion are needed the requirements are generally less stringent. Usually a single additional axis is sufficient to provide a 'hop' in order to move from position to position on a many-faced gauge, e.g. a step gauge. This axis is generally only required to move safely between a measurement position and a safe position with all parts of the probing system outside the gauge structure to allow safe motion of the primary axis. Of these requirements, it is the ability to return to the measurement position accurately and repeatably which is the most critical, especially if a corner cube-based interferometer is used since unpredictable behaviour can occur if the incoming beam hits the focus of the cube and the vertical displacement of the beam will change, potentially causing issues at the detector.

Occasionally a third axis is required to enable variation in length across a measurement face (the flatness of the face) to be assessed. The motion would be expected to be short range but repeatable over that range.

Traditional CMMs meet many, in some cases all, of the requirements for a motion stage able to deliver all that is required for a primary length system, and several such systems in use make use of a CMM as the motion base. These include the step gauge calibration instruments at NPL, CENAM, INMETRO and VSL [30].

Kruger discusses some of the disadvantages of basing a primary calibration system on a CMM [34]. He notes that as a versatile measurement machine it may not ideal to devote a CMM to primary calibration work, in which its measurement capability will not be utilised (primary systems universally use an interferometer to track the probe position of the CMM rather than using the machine's own linear scales) and he also raises concern about temperature stability on a CMM. This second point matches this author's experience with the NPL step gauge rig where the bridge of the CMM shades a section of the measurement axis from the downflowing controlled temperature air and leads to a temperature gradient along the length of the scale that must be compensated for.

The motion base of other instruments utilise classical measurement machines such as a Moore Measuring Machine at INRIM [33] or SIP length measuring machines at LNE and BEV [30]. These classic instruments provide exceptional motion characteristics, are generally well understood and are characterised motions systems. They may also be less in demand for other applications. However, such systems are hard to procure due to the dominance of the CMM in the current marketplace, so a prospective instrument builder may have to look elsewhere. As with CMMs the built-in measurement capability of these instruments is unused in primary calibration applications, making the use of these systems as a motion base less desirable from the point of view of economy and resource utilisation.

Byman *et al* [32] describe the custom built motion system of their step gauge interferometer in detail. The motion system is based on a coarse/fine control principle. First, a long-range coarse positioning system comprising a carriage supported on vacuum preloaded air bearings following a granite linear rail and, driven by a stepper via a linear unit, positions the measurement carriage close to the measurement position. The linkage between the carriage and the probe system is engineered to eliminate forces not required for linear motion. Second, a fine motion system utilising a piezo actuated linear translation stage is used to drive the probing motion of the system.

It is also notable that rather than displacing the probe vertically in order to hop over inserts in step gauges the VTT-MIKES step gauge interferometer instead rotates the probing structure. This leads to the probe rising 13 mm to clear probe

inserts while the positioning of the corner cubes is such that the rotation motion causes no variation of measured interferometer path length.

The coarse/fine principle was also used by Eom *et al* in the KRISS universal end standard calibration system [42]. The coarse stage is similar in configuration to that used by Byman *et al* but is driven by a geared DC motor and a friction wheel. The fine motion, over a range of approximately 39 μm is provided by a multilayer PZT actuator. A vertical stage, using a ball screw driven by a geared DC motor, is used for hopping. Additionally, the angular motion errors of all the stages are actively compensated for by using two PZT driven tilt stages, controlled in a feedback loop by a three-axis laser interferometer. This presents a potential error source as the probing point of the system is not co-incident with the rotation centres of the tilt stages, which means that the compensation of the angular errors causes a translational movement of the probe. Eom *et al* noted this but add that their system usually only produces small angular errors and the correction inherently cancels the translation with the original angular error.

The PTB nanometer comparator uses a single air bearing slide driven by a linear motor to achieve its primary motion. It also uses piezoelectric actuators to actively correct angular errors in the motion and additionally uses these to drive an active Abbe error correction system (see section 3.1).

As always, the safest way to deal with an error is to eliminate it entirely. This is an advantage of direct face interferometry as employed by the NPL Primary length bar interferometer [22], PTB's next generation Kösters interferometer [23] and the NPL-TESA gauge block interferometer [25–27]. These systems usually have moving parts, for example the rotary platen in the gauge block interferometer, but these exert little effect on the measurements to be made. However, this approach, as already noted, is primarily limited to lapped-end single length standards, such as gauge blocks.

3.3. Compensating for air refractive index

A review by Abou-Zeid [43] identifies four principle methods by which the refractive index of air can be determined so that the necessary compensation can be applied, namely: refractometers, the two colour method, empirical equations and acoustic methods. The latter has been reported by Lassila *et al* [44], demonstrating a practical setup using ultrasonic pulses able to achieve a standard uncertainty of refractive index of air in the order 2.6×10^{-8}. This setup presented difficulties at short ranges (0 m–3 m) due to echoes having a significant detrimental effect on the accuracy of the system (errors of $\approx 3 \times 10^{-7}$ in refractive index were observed when a stone table was placed 10 cm below the beams). This is offset against the advantage of measuring the effective refractive index over the whole beam path rather than discrete sampling of the same.

For the shorter ranges typically associated with the primary instrumentation which are the focus of this review, and given that these instruments are generally housed in highly stable environmentally controlled laboratories [45] (as an example, the NPL dimensional laboratories are temperature controlled to 20 °C ± 0.1 °C and humidity controlled to 45%rh ± 5%rh), the majority of primary level 1D instrumentation corrects for refractive index using empirical equations. Most commonly used are the equations derived by Edlén [46], as modified and subsequently corrected by Birch and Downs [47, 48]. Recent instruments developed by Lassila *et al* [27, 32], Picotto *et al* [33, 49], Eom and Han [42] and Sun *et al* [31] all utilise the modified Edlén equations for refractive index compensation. To do this measurements are required of air temperature, pressure, humidity and in some cases carbon dioxide, although standard conditions for the latter are often assumed except for the highest accuracy systems [22].

The Edlén equation remains the most common choice for refractive index compensation, offering an estimated standard uncertainty of 1×10^{-8} for the equation, with a suggestion of a typical uncertainty including sensor uncertainties of 1×10^{-7} [47]. A more recent estimate by Jaeger gives a total uncertainty contribution when using the Edlén equations of 5×10^{-8} though this value will depend on the choice of sensors [50]. However other empirical equations exist and can be used. Ciddor [51] developed equations for refractive index for wavelengths in the visible and near infrared. A custom refractive index measurement unit [52] which uses these equations was utilised by Rerucha *et al* [53] in development of their new diode based stabilised laser source.

Bönsch and Potulski further refined the modified Edlén equation, specifically the humidity term, based on refractometer measurements reporting standard uncertainties of 1×10^{-9} and a total uncertainty for refractive index including sensor uncertainties of 1×10^{-8} for measurement in humid air (the uncertainty in dry air is less) [54]. This work was continued by Chen *et al* [55] who further improved the humidity term by making measurements with three stabilised lasers in a phase step interferometer. This last work reports the highest accuracy of any of the empirical equations, stating that it is superior to that reported by Bönsch and Potulski without giving a numerical value, though as yet no instrument has been reported as utilising it.

The two colour method, using the varying dispersion of two different wavelengths passing through the same path was first developed over 50 years ago [56] and shares the advantage of measuring the full beam path refractive index. The method has been applied to interferometry by various groups [57–60], with work from Wu *et al* [61] using an optical frequency comb achieving an uncertainty change of 5×10^{-8}. A difficulty with the two-colour method is that it does not produce valid results when the air is moist. A solution is to use a third wavelength [62] but this introduces significant scaling factors to the uncertainty calculation which make the method unviable if visible wavelengths are used [43]. Golubev and Chekhovsky proposed a refinement of the three colour method using two harmonics of a YAG:Nd^{3+} laser and a CO_2 laser [63]. This instrument was principally aimed at use over very long ranges (up to 30 km) and was designed as a range finder.

In a study by Dong *et al* [64] the accuracy of two colour methods was compared to the more commonly used empirical

equations for determining the refractive index of air. This study showed that two colour methods could actually exceed the accuracy achieved by empirical equations but only when the air was dry (0%rh). Since this is an undesirable state for precision dimensional measurement due to the risk of static build up the two-colour method is almost, if not entirely, unused for primary level 1D instrumentation in the macroscale range.

The use of refractometers in instruments is limited by practical considerations. It is difficult to ensure that the sample of air measured in the refractometer is representative of the air along the beam path. In particular temperature differences between the beam path and the location of the refractometer can lead to significant differences between the refractive index of the air in the refractometer compared to that in the beam path. Additionally, most refractometers compare the chromatic dispersion of the air to be sampled against vacuum. To do this two chambers of fixed length are used which initially are both filled with air then one is pumped down to vacuum [65]. The time this takes and the added complexity of maintaining the necessary vacuum systems make the use of these types of refractometers impractical for length instruments. In addition, the mechanical changes imposed on a body by evacuating it mean that the fixed length of the chambers is likely to be compromised by the evacuation creating a significant error source.

Other refractometer designs exist which have a permanent vacuum cell. These are unable to provide absolute refractive index measurements. However Decker *et al* used such a system in their next-generation Kösters interferometer for gauge block measurement [23] and a similar setup is reported for PTB's Precision Interferometer [66, 67]. Here a permanently evacuated quartz cell of known length is placed within a measurement arm of the interferometer and the phase of the path through it is compared to the phase of nearby air paths [66]. This does not in itself allow the direct calculation of refractive index but when combined with an estimate of the refractive index from the Bönsch and Potulski modified Edlén equation it is able to provide more accurate determinations of refractive index than a more conventional evacuating refractometer or the empirical equations alone [43].

The layouts described in [42–44] overcome many of the difficulties of using refractometers. The instrument layouts allow the vacuum cell to be placed close to the measurement path, minimising differences in environment. The cell being permanently evacuated avoids mechanical distortions caused by pumping down in a conventional refractometer. However, the optical layouts used are quite restrictive in what can be measured. Only single length artefacts with plane end faces, namely gauge blocks, can be measured in these systems. Applying this technique to other sorts of systems able to measure a wider range of artefacts would be challenging, especially over longer ranges.

An alternative approach to dealing with the issue of measuring the refractive index of air is to remove the air. If the beam path of a measurement system is in vacuum, then no refractive index compensation is necessary. This approach was taken by Flügge *et al* in the design of the PTB Nanometer Comparator [40, 68]. This instrument has expandable vacuum bellows surrounding the beam path of the reference interferometer and the interferometer optics are all held in vacuum so that there is no laser path in air in the measurement position. An auxiliary stage running parallel to the main motion slide compensates for the varying forces of the bellows as they open and close. This instrument claims the lowest uncertainty of any macroscale length instrument in the KCDB and achieving a fully evacuated beam path is a considerable engineering achievement which gives a clear performance advantage to the machine. However, it is unclear how achievable longer measurement ranges might be (the maximum range of the PTB Nanometer Comparator is 610 mm) given the difficulties likely to be met in building longer vacuum bellows.

3.4. Probing techniques and calibration

Probing for 1D instruments will usually take the form of either a tactile probe or a camera system. The latter is used for systems measuring line or other optical standards while end and diameter standards will usually be measured with the former. Exceptions to this general rule are instruments for measuring gauge blocks and length bars which use direct face interferometry. Here the probing system may be considered as the laser light illuminating the faces and the camera system used to obtain the images of the fringe pattern. The laser light is equivalent to the stylus of a conventional probe (it 'touches' the surface) while the camera is the equivalent of the displacement detection sensor, for example a strain gauge in a typical CMM probe.

A number of instruments that use CMMs as the motion system, for example the step gauge calibration systems at NPL, VSL, and CMI [30] also use the probing system of the CMM, in some cases using a customised stylus assembly which includes the interferometer reflectors. A good discussion of the different forms of CMM probes can be found in the NPL good practice guide on CMM probing authored by Flack [69]. From the point of view of 1D instruments the performance of simpler forms of CMM probes are limited by the fact that the probing force generated varies according to the direction of probing and is not equal across any straight line. More accurate systems use strain gauges in place of kinematic mounts which largely eliminate this. The highest accuracy CMMs use analogue probes based on three spring parallelograms. These measure residual deflection of the probe head and can supply this as a correction to measurement data. Such probe heads can also clamp unrequired axes, allowing single dimension probing. However, such probes are expensive and difficult to obtain except as part of a complete CMM.

For self-build machines a commonly used probe is the Cary (Now Tesa) I-Dim probe. This is an inductive probe with a spring providing the return force. Designed to work in 1-dimension this probe is used in LNE's step gauge calibration system [30], the INRIM 1D comparator [33] and the step gauge calibration system at CENAM [30]. This last system has replaced the probe head of the CMM it uses as a motion base with a Cary (Now Tesa) I-Dim probe.

The VTT-MIKES interferometer for step gauge calibration utilises a Mahr 1320/1 inductive probe with the addition of a long ruby tipped stylus to avoid magnetic effects. The probing system is driven by the fine motion piezo stage of this instrument in 100 nm steps toward the measurement face. Twenty measurements of the interferometric position of the probe and probe displacement are made. An extrapolation is then made as to what the measuring face position would be if a zero force probing could be made [32]. This approach is an effective way to avoid issues around compression effects and probe bending as these should be corrected by the extrapolation. However, the relation between the probing force and the face position becomes more complex as the probing force nears zero and various surface effects become significant [70]. In this domain data generated may show non-linearity with respect to the profile generated at higher forces. Byman *et al* reported that they discard data taken with a probe bend of less than 0.5 μm for this reason [32]. Eom and Han also reported using a bi-directional inductive probe on the KRISS linear measuring system (the manufacturer and type is not reported) [42]. The particular probe they use has a large offset between zero positions in the forwards and backwards positions and has a large probing force. They suggest that improvement could be made by use of a parallelogram type inductive probe.

This system also features an optical probing system which uses a microscope and CCD camera for measurement of line scales. Similar optical systems are used by the MIKES fibre-coupled differential dynamic line scale interferometer [71], the PTB nanometer comparator [37] and the large majority of participants in the EURAMET.L-K7.2006 line scale comparison exercise (the exceptions either used a microscope centring by eye rather than by electrical means or did not report their method) [72]. At present no alternative methods for measuring line scales appear to be in use for primary calibration systems at the highest levels of performance. This implies that the CCD camera/microscope, or alternatively the photo-electric microscope is a mature technology for this application.

Returning to tactile probing systems, those which make bidirectional measurements must make a measurement of the effective diameter of their probing system. In the VTT-MIKES interferometer for step gauge calibration, effective diameter of the probe tip is calibrated using a calibrated gauge block [32], in common with almost all of the tactile probe equipped instruments discussed so far in this review. Since gauge blocks are the end standard able to be calibrated with the smallest uncertainty this choice is logical. VTT-MIKES also use a gauge block stack to create an internal gap distance as an additional verification. This is similar to the approach used by the NPL internal diameter machine. Here, fused silica box standards have been produced and the gap width is calibrated using a white light interferometer. The box standards are then used to qualify the probe diameter prior to the measurement of a ring gauge [29].

A key advantage of calibrating the probe in this manner is that the measurement of effective diameter includes elastic compression, so provided the material properties of the gauge block and the artefact under calibration are the same the elastic compression can be largely cancelled out. Even if the materials are different, at low probing forces the difference in compressions will generally be a significantly smaller term than the uncorrected compression.

A subset of tactile devices, usually used for diameter measurements, may have two probes which will contact either side of the standard. The PTB KOLD instrument (Comparator for length and diameter) developed by Jusko and Hesse uses a probing arrangement of this type [73]. The instrument is built from two Mahr Cylinder form and roundness instruments with a common rotary table. The probes of the two instruments are offset in such a way that the two probes can be brought into direct contact with each other. This allows the interferometer to be zeroed with the two probes touching and then the probes are moved apart to contact the surface of the diameter standard under calibration. This setup effectively calibrates out the probe diameter from the measurement but can only function on artefacts where the calibrated lengths are defined between opposing faces. It also requires a complex probe configuration to enable the probes to contact both their inside and outside faces, enabling both internal and external diameters to be calibrated.

3.5. Temperature systems

Comparatively few of the primary length measuring instruments include their own dedicated temperature control. Most of such equipment relies on the environmental controls of the laboratory in which it is located. Environments with temperature stability of better than 20 °C ± 0.1 °C can be achieved in this way [45]. However, the infrastructure required is both complex and costly and these factors increase significantly as the specification on temperature tightens.

A method to achieve better performance with a lower infrastructure cost is to temperature control a smaller enclosure around the instrument. The NPL primary length bar interferometer uses such an enclosure to achieve a temperature stability of 20 °C ± 0.03 °C. The casing is built with a weave of water pipes enclosed in the baseplate and lid of the structure. Temperature controlled water from a precision temperature bath is pumped through the pipework to maintain the environment. The temperature of the bath is controlled based on measurements of the baseplate temperature measured using platinum resistance thermometers (PRTs) [22]. The KRISS universal end standard calibration system also uses a thermal control case, with liquid cooling built in. The reported results show this achieving a temperature stability of 20 °C ± 0.02 °C [36].

Platinum resistance thermometers (PRTs) are the most widely used thermal sensor among the instruments reviewed so far in this paper. This is due to the higher accuracy and stability of such devices. Kim *et al* used thermistors on the KRISS Abbe-type comparator [28]. These give an advantage of a faster response time and greater sensitivity but the reduction in accuracy and greater long-term variation has generally led to the favouring of PRTs. However, there are issues with how PRTs are used within dimensional metrology, particularly for

the measurement of air temperature in refractive index compensation. The diameter of the probe used can significantly affect the magnitude of radiative error in the thermometer and the low air flow found in many dimensional laboratories to minimise turbulence may mean that objects, including thermometers, are more strongly radiatively coupled to the walls and ceiling of a room than they are thermally coupled to the air [74]. For this reason, de Podesta *et al* recommend consideration of multiple sensor approaches with thermistors and thin form thermocouples working alongside PRTs.

Acoustic thermometry is a developing field of great potential for accurate thermometry, but it has yet to be taken up by the dimensional community. Korpelainen and Lassila made thermal measurements as part of their acoustic method for determining refractive index but noted that echos from the the structure of the measurement instrument results in errors that were sufficient to leave the system less accurate than contact thermometry methods [44].

4. Discussion

It is apparent from the range of approaches that there is no single ideal design for primary length instrumentation. Rather, differing priorities or restrictions drive design decisions and lead to varying approaches ready to achieve the same tasks. This variation can be seen as a strength of the global system of measurement as it avoids biasing length measurement traceability with the errors, including potential unknown errors, of a single instrument design. However, it also limits the standardisation of measurement potentially leading to variation, although such variation should always be within the claimed uncertainty of measurement of the instruments.

It should be noted that the variation of design is largely absent in gauge block metrology where the NPL-TESA gauge block interferometer and the Kösters type interferometer dominate. Here it appears that hardware design has matured although several institutes have developed their own control and analysis software. It is also notable that the NPL-TESA gauge block interferometer is one of very few instruments covered in this review that is commercially available.

Probing technology for the optical probing of line standards has also matured with the use of optical microscopes with photoelectric sensors now being ubiquitous. Improved imaging processing and higher resolution detectors may be areas where future development of these systems can seek greater performance.

Refractive index compensation is another area where a single solution is universally adopted. While alternatives to empirical equations exist and are in use for longer range systems, all macroscale primary systems in use, excepting those that operate interferometry in vacuum, utilise an empirical equation approach for determining refractive index of air. Most systems still use the Birch and Downs modified Edlén equations despite more recent research which claims to have improved on the accuracy of these equations. This may be due to the fact that the modified Edlén equations are tried and trusted and, while the new equations offer an improvement, the differences are small enough that the additional effort of implementing the new equations may not be justified.

Given that temperature effects are typically the dominant uncertainty term it is surprising that relatively few instruments have local temperature control as part of their system. Certainly, this is something which future designers may want to consider, especially as controlling the environment of whole laboratories is far more energy intensive and environmental concerns are increasingly becoming important to instrument buyers and users. Constructing the instrument from low thermal expansion materials can avoid some of the temperature issues but as already discussed this brings further challenges, not least of which is cost, while not addressing all of the errors caused by varying temperature (change in refractive index and the thermal expansion of the artefact under test would not be helped in this way). It is noted that almost all instruments discussed in this review utilise platinum resistance thermometry exclusively but concerns about radiative effects on these devices, especially for air temperature measurements may lead to a view that multiple sensor technologies should be considered going forward.

Pursuing excellence in thermometry will always pay dividends for the dimensional instrument designer.

In other areas technologies and strategies adopted vary considerably. With motion stages it is notable that older instruments such as universal measuring machines are being repurposed by laboratories with access to them. This may be in part due to cost constraints on development (it being cheaper to repurpose an existing system than to procure a new one) but is also a reflection on the excellence of the engineering of these systems, producing motion of sufficiently low error that more modern motion stages have not yet rendered them obsolete.

One common theme from the motion control, although not universal, was the adoption of the coarse/fine control concept for the motion controllers. While some instruments are designed with a primary control system of high enough resolution to avoid this, including most notably the PTB nanometer comparator, the majority added a second system, typically a piezo device for the finely controlled short-range motion.

Dealing with Abbe error shows clearly how an apparently simple concept can nonetheless be very complex to overcome. A great variety of layouts and compensation methods are used with the optimum method being highly dependent on other design factors, such as the maximum range of the instrument, laboratory space available, probe mass constraints and achievable interferometry setups. As each of these parameters will vary for individual instruments and laboratories it is not possible to define an optimum method of overcoming Abbe error, and the uncertainty performances of different instruments do not support there being a single optimum method either, with very different configurations achieving similar performance levels. The approach of a primary level calibration instrument designer to the Abbe principle should then be governed by the method that best suits other aspects of the design.

Likewise, the choice of tactile probing systems is largely governed initially by other aspects of the instrument configuration, in particular the choice of motion stage. Where this does not dictate the approach to be taken then commercial

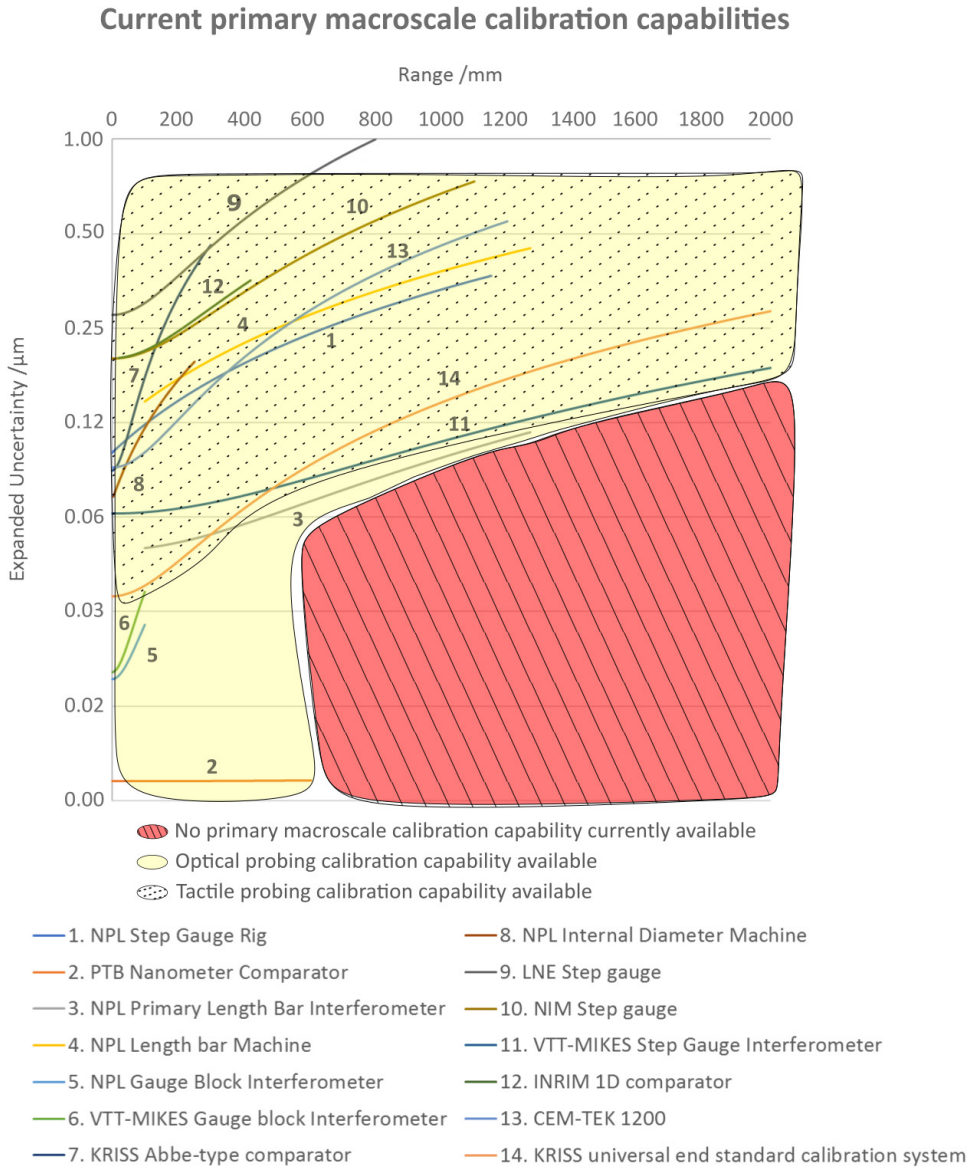

Figure 5. Measurement capabilities of instruments reviewed in this paper. Uncertainties plotted on a log scale axis versus range (linear axis).

probes appear to be preferred to custom design, in contrast to other systems where bespoke development is more usual. This shows that the commercially available technologies are sufficiently high performance that any improvements made through bespoke design would produce a marginal improvement to overall instrument performance. As a result, design effort is placed into other factors.

However, it is notable that tactile probing instruments are currently unable to achieve the low uncertainties currently achieved by some optical detection systems (see figure 5). The full reasons behind this require additional investigation but it is certainly true that most of the tactile probing systems reviewed are reliant on a calibrated article, often a gauge block, which was calibrated using an optical probing system such as a gauge block interferometer, for measuring the effective probe diameter. This represents an uncertainty limit for tactile probing-based instruments. The development of techniques to avoid this requirement may help to fill this capability gap.

Among these other factors will be aspects such as usability, maintainability and software control systems, which while beyond the scope of this review are of course critical design factors. Best practice in these areas is well covered, in literature and in industry standards. The purpose of this review is to act as a starting point to help the prospective designer of a primary level 1D calibration system to gain insights into how their peers have approached the challenge of overcoming the major application specific design challenges that they will face and find ideas and strategies that can form the basis of new improved instruments that will advance the performance of dimensional metrology to meet the needs of science, industry and wider society, in areas such as additive manufacturing, ultra-precision engineering, medical technologies, aerospace manufacturing and the automotive industry to name only a few.

The challenge facing primary dimensional metrology is to be an enabler to these and other sectors in the decades to come by ensuring that the measurement capability exists to support the ever-increasing demand for tighter precision and better accuracy in length measurement on the shop floor. Figure 5 shows the current measurement capabilities of the instruments reviewed in this paper. It can clearly be seen that there is a large capability gap at longer ranges and low uncertainties. Taniguchi showed projected improvements in manufacturing capabilities [75] and from this it can be seen that this capability gap could soon be a constraining factor on further improvements in manufacturing.

To avoid this enabling capability NMI level calibration must continue to improve, in particular seeking to fill the capability gaps shown, as this represents the ultimate limit of traceable measurement performance.

Acknowledgments

The author acknowledges funding from the UK Department for Business, Energy and Industrial Strategy (BEIS) as part of the National Measurement System Programme.

ORCID iDs

Tim Coveney https://orcid.org/0000-0002-2967-2324

References

[1] Bureau International des Poids et Mesures and Organisation Intergouvernementale de la Convention du Mètre 2019 *Le Système international d'unités (SI) The International System of Units (SI)* 9th edn (Paris: Bureau international des poids et measures)
[2] CCL 2019 Mise en pratique—metre—Appendix 2—SI Brochure www.bipm.org/utils/en/pdf/si-mep/SI-App2-metre.pdf (Accessed: 11 June 2019)
[3] Bureau International des Poids et Mesures 2018 BIPM—Recommended values of standard frequencies www.bipm.org/en/publications/mises-en-pratique/standard-frequencies.html (Accessed: 27 March 2018)
[4] ISO 3650:1999 *Geometrical Product Specifications (GPS)—Length standards—Gauge blocks* (International Organization for Standardization)
[5] BS 5317: 1976 Specification for Metric length bars and their accessories (British Standards Institution) pp 1–16
[6] Koba 2018 Fabrik für Präzisions-Messzeuge—Precision Step Gauge KOBA-step and KOBA-step mini www.koba.de/en/products/artifacts-for-3-coordinate-measuring-machines/precision-step-gauge-koba-step-and-koba-step-mini.html (Accessed: 10 July 2018)
[7] Mitutoyo 2019 Product: High Accuracy Check Master https://shop.mitutoyo.co.uk/web/mitutoyo/en_GB/mitutoyo/1291712680712/HighAccuracy Check Master/$catalogue/mitutoyoData/PR/515-743/index.xhtml (Accessed: 10 July 2018)
[8] BS 4064:1966 Specification for Plain setting rings for use with internal diameter measuring machines—Metric units (British Standards Institution)
[9] BS 1044-1:2008 Specification for gauge blanks Part 1: Plug, ring and calliper gauges (British Standards Institution)
[10] BIPM 2018 The BIPM key comparison database https://kcdb.bipm.org/ (Accessed: 27 March 2018)
[11] BIPM 2019 Key comparison database—Line Scale CMCs for Germany www.bipm.org/exalead_kcdb/exa_kcdb.jsp?_c=+16366751034942705708/_c=+15223228926863566409&_C=eJw9yEEOQEAMRuH∗KI6AGzBiY!kAzYQm06SqDOL4wsLm5csjBRvoMgyha6lxZ5vlDqDVD1kto∗o5ctyn9I7oKEG6vPavG1SMizxFZVCSoz9VUZd4AOA6Hc4_&_p=AppC (Accessed: 29 January 2019)
[12] Hale L C 1999 Principles and techniques for designing precision machines *PhD Thesis* Lawrence Livermore Laboratory, University of California
[13] Pulfrich C 1892 Üeber einige von Professor Abbe konstruirte Messapparate für Physiker *ZfI* **12** 307–15 (in German)
[14] Stone J A A, Decker J E E, Gill P, Juncar P, Lewis A, Rovera G D D and Viliesid M 2009 Advice from the CCL on the use of unstabilized lasers as standards of wavelength: the helium–neon laser at 633 nm *Metrologia* **46** 11–8
[15] Flack D and Hannaford J 2005 *Measurement Good Practice Guide: Fundamental Good Practice in Dimensional Metrology* No. 80
[16] Puttock M J and Thwaite E G 1969 Elastic compression of spheres and cylinders at point and line contact *National Standards Laboratory Technical Paper* No. 25
[17] ISO 1:2016 Geometrical product specifications (GPS)—Standard reference temperature for the specification of geometrical and dimensional properties (International Organization for Standardization)
[18] Schott 2016 ZERODUR® Extremely Low Expansion Glass Ceramic: SCHOTT advanced optics|SCHOTT AG *Schott Ag* www.schott.com/advanced_optics/english/products/optical-materials/zerodur-extremely-low-expansion-glass-ceramic/zerodur/index.html (Accessed: 13 July 2017)
[19] Berthold I I I J W, Jacobs S F and Norton M A 1977 Dimensional stability of fused silica, invar, and several ultra-low thermal expansion materials *Metrologia* **13** 9–16
[20] Bryan J P 1979 The Abbe principle revisited: an updated interpretation *Precis. Eng.* **1** 129–32
[21] Zhang G X 1989 A study on the Abbe principle and Abbe error *CIRP Ann. Manuf. Technol.* **38** 525–8
[22] Lewis A 1994 Measurement of length, surface form and thermal expansion coefficient of length bars up to 1.5 m using multiple-wavelength phase-stepping interferometry *Meas. Sci. Technol.* **5** 694–703
[23] Decker J E, Schödel R, Bönsch G, Schodel R and Bonsch G 2003 Next-generation Kösters interferometer *Proc. SPIE* **5190** 5110–90
[24] Rau K, Mai T and Schödel R 2014 Absolute length measurement of prismatic bodies with PTB's new double-ended interferometer under the influence of wavefront aberrations *Proc. MacroScale* pp 1–9
[25] Pugh D J and Jackson K 1986 Automatic gauge block measurement using multiple wavelength interferometry *Proc. SPIE* **656** 244–9
[26] Lewis A J, Hughes B and Aldred P J E 2010 Long-term study of gauge block interferometer performance and gauge block stability *Metrologia* **47** 473–86
[27] Byman V and Lassila A 2015 MIKES' primary phase stepping gauge block interferometer *Meas. Sci. Technol.* **26** 084009
[28] Kim J-A, Kim J W, Kang C-S and Eom T B 2010 An interferometric Abbe-type comparator for the calibration of

internal and external diameter standards *Meas. Sci. Technol.* **21** 75109
[29] Flack D 1993 The NPL internal diameter machine *Laser Metrology and Machine Performance* (London: NPL)
[30] Prieto E *et al* 2012 Final report on inter-RMO key comparison EUROMET.L-K5.2004: calibration of a step gauge *Metrologia* **49** 4008
[31] Sun S, Shen X, Zou L, Gao H and Ye X 2014 A novel measuring device for step gauge *7th Int. Symp. Advanced Optical Manufacturing and Testing Technologies: Design, Manufacturing, and Testing of Micro- and Nano-Optical Devices and Systems* vol 9283 p 92830D
[32] Byman V, Jaakkola T, Palosuo I and Lassila A 2018 High accuracy step gauge interferometer *Meas. Sci. Technol.* **29** 1–14
[33] Picotto G B, Bellotti R, Pometto M and Santiano M 2011 The INRIM 1D comparator with a new interferometric set-up for measurement of diameter gauges and linear artefacts *MacroScale 2011* pp 1–4
[34] Kruger O A 2001 An investigation into the measuring of the length spacing of step gauges *Proc. SPIE* **4401** 70–82
[35] Prieto E and Rodriguez J 2003 New capabilities of the CEM-TEK 1200 interferometric comparator for calibrating long gauges, step gauges and now line scales *Proc. SPIE* **5190** 80–92
[36] Kim J-A, Kim J W, Kang C-S, Jin J and Eom T B 2011 An interferometric calibration system for various linear artefacts using active compensation of angular motion errors *Meas. Sci. Technol.* **22** 75304
[37] Flügge J, Köning R, Schötka E, Weichert C, Köchert P, Bosse H and Kunzmann H 2014 Improved measurement performance of the Physikalisch-Technische Bundesanstalt nanometer comparator by integration of a new Zerodur sample carriage *Opt. Eng.* **53** 122404
[38] Köning R, Flügge J and Bosse H 2007 Achievement of sub nanometer reproducibility in line scale measurements with the nanometer comparator *Proc. SPIE* **6518** 65183F
[39] Flügge J, Köning R, Weichert C, Vertu S, Wiegmann A, Elster M S C, Schulz M and Bosse H 2009 The PTB Nanometer Comparator for metrology on length graduations and incremental length encoder systems *ISMTII 2009* pp 97–101
[40] Flügge J, Weichert C, Hu H, Köning R, Bosse H, Wiegmann A, Schulz M, Elster C and Geckeler R D 2008 Interferometry at the PTB Nanometer comparator: design, status and development *Proc. SPIE* **7133** 713346
[41] Köning R, Flügge J and Bosse H 2007 A method for the *in situ* determination of Abbe errors and their correction *Meas. Sci. Technol.* **18** 476–81
[42] Eom T B and Han J W 2001 A precision length measuring system for a variety of linear artefacts *Meas. Sci. Technol.* **12** 698–701
[43] Abou-Zeid A 2015 Refractive index of air for interferometric length measurements *Proc. 2015 Int. Symp. Precision Engineering Measurement* vol 9446 p 944640
[44] Korpelainen V and Lassila A 2004 Acoustic method for determination of the effective temperature and refractive index of air in accurate length interferometry *Opt. Eng.* **43** 2400
[45] Lassila A *et al* 2011 Design and performance of an advanced metrology building for MIKES *Measurement* **44** 399–425
[46] Edlén B 1966 The refractive index of air *Metrologia* **2** 71–80
[47] Birch K P and Downs M J 1993 An updated Edlén equation for the refractive index of air *Metrologia* **30** 155–62
[48] Birch K P P and Downs M J J 1994 Erratum: correction to the updated Edlén equation for the refractive index of air (Metrologia (1994) 31 (315-316)) *Metrologia* **31** 315–6
[49] Bellotti R, Franco M, Picotto G B and Pometto M 2014 Renewal of the gage-block interferometer at INRIM *Proc. MacroScale* pp 1–5
[50] Jaeger G 2010 Limitations of precision length measurements based on interferometers *Measurement* **43** 652–8
[51] Ciddor P E 1996 Refractive index of air: new equations for the visible and near infrared *Appl. Opt.* **35** 1566–73
[52] Hucl V *et al* 2013 Automatic unit for measuring refractive index of air based on Ciddor equation and its verification using direct interferometric measurement method *Proc. SPIE* **8788** 878837–39
[53] Rerucha S, Yacoot A, Pham T M, Cizek M, Hucl V, Lazar J and Cip O 2017 Laser source for dimensional metrology: investigation of an iodine stabilized system based on narrow linewidth 633 nm DBR diode *Meas. Sci. Technol.* **28** 045204
[54] Bonsch G and Potulski E 1998 Measurement of the refractive index of air and comparison with modified Edlén's formulae *Metrologia* **35** 133–9
[55] Chen Q, Liu J, He Y, Luo H, Luo J and Wang F 2015 Humidity coefficient correction in the calculation equations of air refractive index by He–Ne laser based on phase step interferometry *Appl. Opt.* **54** 1109
[56] Bender P L and Owens J C 1965 Correction of optical distance measurements for the fluctuating atmospheric index of refraction *J. Geophys. Res.* **70** 2461–2
[57] Pavese F 2009 About the treatment of systematic effects in metrology *Measurement* **42** 1459–62
[58] Matsumoto H and Honda T 1992 High-accuracy length-measuring interferometer using the two-colour method of compensating for the refractive index of air *Meas. Sci. Technol.* **3** 1084–6
[59] Meiners-Hagen K and Abou-Zeid A 2002 Two colour interferometer with compensation of refractive index of air *Photonics Meas.* **1694** 125–30
[60] Kuschmierz R, Czarske J and Fischer A 2014 Multiple wavelength interferometry for distance measurements of moving objects with nanometer uncertainty *Meas. Sci. Technol.* **25** 85202
[61] Wu G, Arai K, Takahashi M, Inaba H and Minoshima K 2013 High-accuracy correction of air refractive index by using two-color heterodyne interferometry of optical frequency combs *Meas. Sci. Technol.* **24** 15203
[62] Rank D H, Saksena G D and McCubbin T K 1958 Measurements of the dispersion of air from 3651 to 15 300 Angstroms *J. Opt. Soc. Am.* **48** 455–8
[63] Golubev A N and Chekhovsky A M 1994 Three-color optical range finding *Appl. Opt.* **33** 7511–7
[64] Wei D, Takamasu K and Matsumoto H 2016 Is the two-color method superior to empirical equations in refractive index compensation? *Opt. Photonics J.* **06** 8–13
[65] Schellekens P, Wilkening G, Reinboth F, Downs M J, Birch K P and Spronck J 1986 Measurements of the refractive index of air using interference refractometers *Metrologia* **22** 279–87
[66] Schoedel R and Boensch G 2003 Precise interferometric measurements at single-crystal silicon yielding thermal expansion coefficients from 12° to 28°C and compressibility *Recent Dev. Traceable Dimens. Meas.* **4401** 54
[67] Schödel R and Abou-Zeid A 2009 High accuracy measurements of long-term stability of material with PTB's precision interferometer **7133** 71333J
[68] Flügge J and Köning R 2001 Status of the nanometer comparator at PTB *Proc. SPIE* **4401** 275–83

[69] Flack D 2014 *Good Practice Guide No. 43: CMM Probing*
[70] Claverley J D, Georgi A and Leach R K 2010 Modelling the interaction forces between an ideal measurement surface and the stylus tip of a novel vibrating micro-scale CMM probe *IFIP Advances in Information and Communication Technology* vol 315 (Teddington: National Physical Laboratory) pp 131–8
[71] Lassila A 2012 MIKES fibre-coupled differential dynamic line scale interferometer *Meas. Sci. Technol.* **23** 94011
[72] Acko B 2012 Final report on EUROMET Key Comparison EUROMET.L-K7: calibration of line scales *Metrologia* **49** 4006
[73] Jusko O and Hesse C 2017 A Pseudo-Abbe comparator and double form measurement machine for high precision diameter and form calibrations *Proc. Manuf.* **13** 466–71
[74] de Podesta M, Bell S and Underwood R 2018 Air temperature sensors: dependence of radiative errors on sensor diameter in precision metrology and meteorology *Metrologia* **55** 229–44
[75] Taniguchi N 1983 Current status in, and future trends of, ultraprecision machining and ultrafine materials processing *CIRP Ann. Manuf. Technol.* **32** 573–82